Exp Tech (2017) 41:237–249
DOI 10.1007/s40799-017-0172-7

Reliability Assessment of Real-time Hybrid Simulation Under Worst-Case Scenarios Using Frequency-Domain Evaluation Indices

W. Xu[1] · C. Chen[2] · T. Guo[1] · X. Yang[3]

Received: 6 June 2016 / Accepted: 31 January 2017 / Published online: 13 February 2017

Abstract Real-time hybrid simulation (RTHS) allows researchers to physically evaluate critical parts of a prototype structure at full scale in the laboratory while the rest is numerically modeled. The reliability of the RTHS experimental results however still remains unsolved in the presence of experimental errors even though a number of methods have been proposed based on the actuator tracking in the time domain. Frequency-domain evaluation indices (FEI) provide a novel and effective technique to evaluate the amplitude and phase errors of the actuator tracking. In this paper, the correlation between the reliability of RTHS results and the FEI indices is explored for the worst-case scenarios of single-degree-of-freedom (SDOF) linear elastic structures. The influence of natural frequency and damping ratio are considered through a suite of ground motions. The relationship between the FEI parameters and the error of RTHS replicating actual structural response is explored and a criterion based on worst-case scenarios is proposed for reliability assessment. Numerical simulations are conducted to demonstrate the effectiveness of the proposed reliability criterion.

Keywords Real-time hybrid simulation · Frequency domain evaluation index · Reliability assessment · Probability and statistical methods · Worst-case scenario

✉ T. Guo
Guotong77@gmail.com

[1] Key Laboratory of Concrete and Prestressed Concrete Structures of the Ministry of Education, Southeast University, Nanjing, People's Republic of China 210096

[2] School of Engineering, San Francisco State University, San Francisco 94132, USA

[3] Department of Civil Engineering, Nanjing University of Aeronautics and Astronautics, Nanjing 210016, People's Republic of China

Introduction

With the development of technologies, new innovative rate-dependent materials, such as vibration isolation bearing [1] and elastomeric damper [2], become widely used in building design for seismic hazard mitigation. Laboratory tests are necessary to experimentally assess the performance of these materials when applied in building design. Since external loading is often applied in extended time scale in conventional hybrid simulation, shaking table test seems more appealing for rate-dependent materials [3, 4]. However, due to the capacities of shaking table facilities, full-scale test is often difficult if not impossible in laboratories. Real-time hybrid simulation technique is developed from conventional quasi-static hybrid simulation [5], but requires that the command displacements be imposed onto the experimental substructure(s) by the actuator(s) in a real-time manner. The dynamics of individual substructures are integrated by an integration algorithm such as central difference method [5], operator-splitting technique (OS) [6] and unconditionally stable explicit CR integration algorithms [7]. Thus, real-time hybrid simulation provides an efficient experimental technique to evaluate the performance of rate-dependent material in large or full scale in size limited laboratories.

The differences between command and measured displacements are inevitable for actuators due to inherent servo-hydraulic dynamics [8–10]. These differences are often referred to as time delay or actuator delay. Time delay has little influence on conventional quasi-static hybrid simulation but

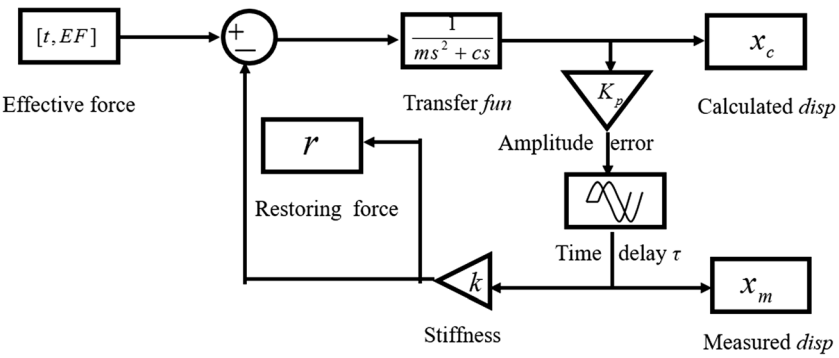

Fig. 1 Block diagram for computational simulations

can be significantly detrimental for real-time hybrid simulation. Actuator delay varies for many different factors such as the structure stiffness and the PID (proportional-integral-derivative) gains in the servo-hydraulic controller. A number of compensation methods have been proposed to minimize the effect of actuator delay in order to achieve good actuator control for real-time hybrid simulation, such as the polynomial extrapolation method [8], linear acceleration extrapolation [11] and the inverse compensation method [10]. These compensation methods require an accurate estimate of actuator delay in the servo-hydraulic system, which is often difficult to acquire before the test. To overcome this, compensation methods based on adaptive control theory have been explored, such as online delay estimation method [12], adaptive inverse compensation (AIC) method [13, 14], the feedforward-feedback tracking control [15] and adaptive time series compensator [16].

However, experimental results showed that the actuator delay can be reduced but cannot be completely eliminated even when a most sophisticated compensation method is used [10]. Post-test actuator tracking assessment is therefore necessary to ensure that the real-time hybrid simulation results truthfully replicate the actual structural responses under earthquakes. Since the actual response is often not available before or even after the test, the calculated displacements from the integration algorithm are often used in comparison with the measured displacements. The maximum tracking error (MTE) and root-mean-square (RMS) [13] are the two often used errors when comparing the calculated and measured displacements. Energy error [17] calculates the energy introduced by the actuator tracking error to estimate the reliability of the test. Tracking indicator (TI) [18] computes the area enclosed by calculated displacements and measured displacements during the test. The phase and amplitude error indices (PAEI) [19] further extends the tracking indicator by fitting the area into an ellipse to get the phase error and amplitude error. These time-domain methods are useful when applied to compare performances of different delay compensation methods for the same experimental setup, but are not practical when applied for tests with different ground motion inputs since structural responses vary under different excitations. Meanwhile, assuming calculated displacements as actual responses is considered inappropriate for time-domain methods since errors in real-time hybrid simulation often accumulate thus deviating the calculated displacements from the actual responses.

More recently, a frequency-domain evaluation index (FEI) was proposed to overcome the disadvantages of existing time-domain techniques [20]. Two indices, i.e., A and ϕ, from frequency domain analysis enable interpreting actuator tracking error in terms of amplitude and phase errors, respectively. The difference between A and 1 denotes the amplitude error, while the difference between ϕ and 0 represents the phase error. More accurate actuator control is achieved when A is closer to 1 and ϕ is closer to 0. By introducing the concept of equivalent frequency, an equivalent time delay d can be calculated for the entire duration of the real-time hybrid simulation, which provides an overall evaluation of actuator control.

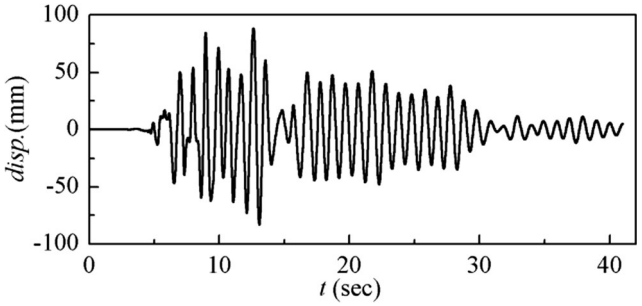

Fig. 2 Actual structural response without amplitude error and time delay

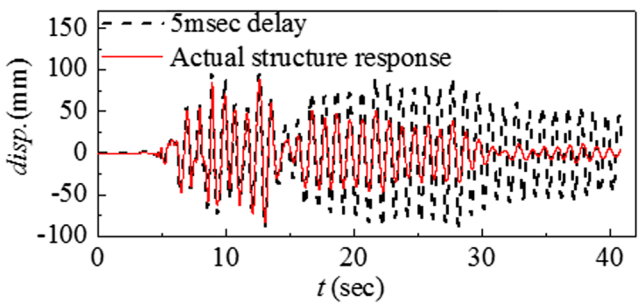

Fig. 3 The measured displacements for time delay of 5msec

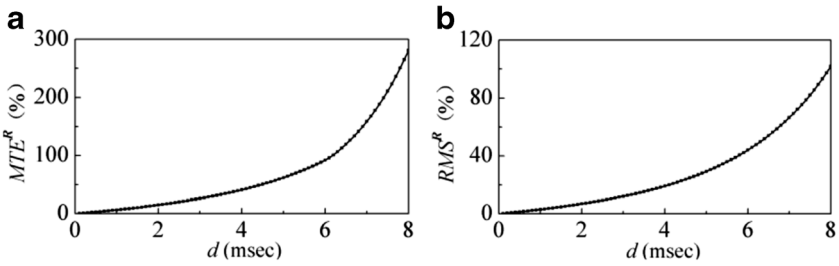

Fig. 4 The relationship between d and error for (**a**) MTE^R and (**b**) RMS^R

Data and frequency decimation were further discussed to improve the efficiency of computation for online evaluation [21].

However, the above mentioned methods in both time and frequency domains can only assess the actuator tracking error during the real-time hybrid simulation, cannot measure the reliability of the test in terms of how truthfully it replicates the actual structural responses under earthquakes. Stability analysis has attracted considerable interests for real-time hybrid simulation when actuator delay exists due to servo-hydraulic dynamics. Wallace et al. [9] used a delay differential equation model to perform stability analysis for real-time hybrid simulation of a single-degree-of-freedom (SDOF) linear elastic structure. The stability limits were calculated as well as the critical delay for linear elastic structures. Wu et al. [6] investigated the effect of actuator delay on real-time hybrid simulation for SDOF linear elastic structure when the operator-splitting (OS) method is utilized for solving the structural dynamics. Chen and Ricles [10] took into account the properties of different explicit integration algorithms and the actuator delay in stability analysis utilizing the discrete transfer function approach. Gao et al. [22] analyzed four different cases for real-time hybrid simulation, in which the worst-case scenario is that the mass concentrates in the numerical substructure and the stiffness concentrates in the experimental substructure. The maximum allowable delay limit was then calculated for a linear elastic system under worst-case scenario. Mercan and Ricles [23] conducted a stability analysis for real-time pseudodynamic and hybrid pseudodynamic testing, which a mapping technique that transforms the characteristic equation of the time delay system into a polynomial. Zhu et al. [24], adopted a discrete-time root locus technique to investigate the delay-dependent stability in RTHS. Maghareh et al. [25] proposed a predictive stability indicator (PSI) due to systematic experimental errors for a SDOF system. This indicator was further extended to MDOF system by converting a delay differential equation to a generalized eigenvalue problem by Maghareh et al. [26].

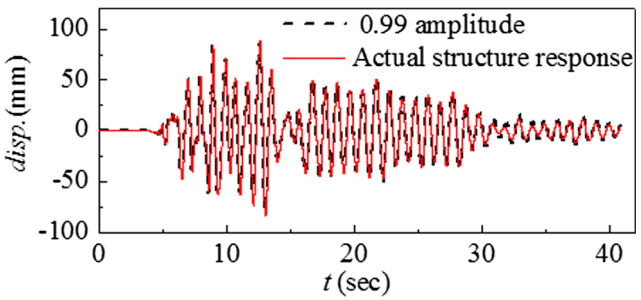

Fig. 5 The measured displacements for amplitude error of 0.99

In this study, the worst-case scenario concept is applied for reliability assessment of real-time hybrid simulation. The reliability of RTHS in this paper represents whether the RTHS results can be used to appropriately interpret the structural performance under earthquakes with the presence of unavoidable test error. In addition, this study will account for amplitude error previously observed in real-time hybrid simulations in laboratories, which is often ignored in previous stability analyses described above. Unlike the stability analysis of real-time hybrid simulation under actuator delay, its accuracy varies for different ground motion inputs. Correlation between FEI indices and the reliability of real-time hybrid simulation is explored for a suite of ground motions.

Frequency-Domain Evaluation Index

The FEI developed by Guo et al. [20] can be briefly described as following. Considering that F[$o(t)$] and F[$I(t)$] represent the Fast Fourier transforms (FFT) of the input and output signals after window transform [27], the weight of ith frequency is defined as,

$$w_i = \frac{\left\| \mathrm{F}[I(t)]_i \right\|^2}{\sum_{i=1}^{p} \left\| \mathrm{F}[I(t)]_i \right\|^2} \tag{1}$$

where $\|\cdot\|$ represents the modulo operation and p represents the number of frequencies to be considered, which equals to half of the smallest power of two that is greater than or equals to the number of data points.

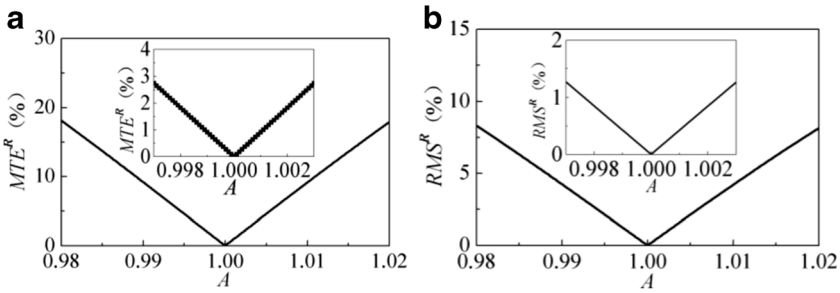

Fig. 6 The relationship between d and test error for (**a**) MTE^R and (**b**) RMS^R

The frequency evaluation index (FEI) between the window transformed input and output is calculated as

$$FEI = \sum_{j=1}^{p} \left\{ \frac{\mathrm{F}[O(t)]_j}{\mathrm{F}[I(t)]_j} \cdot w_j \right\} \tag{2}$$

Then, the amplitude (A) and the phase angle (ϕ) are calculated as follows,

$$A = \|FEI\| \tag{3a}$$

$$\phi = arc\tan[\mathrm{Im}(FEI)/\mathrm{Re}(FEI)] \tag{3b}$$

where $Im(.)$ and $Re(.)$ represent the imaginary and real part of FEI, respectively. The parameter A gives the ratio between the weighted amplitudes of the input and output signals; while the parameter ϕ is the phase difference between the two. The difference between A and 1 is referred to as amplitude error and the value of ϕ is referred to as phase error. To calculate the time delay, the equivalent frequency f^{eq} is defined as,

$$f^{eq} = \sum_{i=1}^{p} (w_i \cdot f_i) \tag{4}$$

The equivalent time delay is then calculated as,

$$d = -\phi \Big/ (2\pi \cdot f^{eq}) \tag{5}$$

Test error, including time lags and coupled dynamics, can be divided into time delay and amplitude error through FEI.

Correlation Between Simulation Accuracy and FEI Indices

The relative MTE (referred as MTE^R) and RMS (referred as RMS^R) are used to assess the difference between actual structural responses and measured displacements from real-time hybrid simulations. Different from measured displacements during the real-time hybrid simulation, the actual structural responses are the displacements derived from computational simulation without any amplitude error or time delay, which are not measurable since the actual responses are not known before or after the test. Due to the cumulative effect of the tracking errors between the command displacements sent to the actuators and the measured displacements from the actuator on RTHS, the global response errors (MTE^R and RMS^R) are not equal to the tracking errors. Nonlinear structural behavior could present a more complicated challenge due to different nonlinearity modeling. Meanwhile, it has been shown by Chen et al. [28] that the yielding behavior of the structure introduces hysteretic damping thus helping stabilize the real-time hybrid simulation, which implies that the linear elastic case is more demanding than the corresponding nonlinear case. To present the methodology of reliability assessment for worst-case scenario, a linear elastic structure is therefore used in this study.

Worst-Case Scenario for Real-Time Hybrid Simulation with Error

The equation of motion for a linear elastic SDOF structure under worst case in real-time hybrid simulation can be expressed as

$$\ddot{x}(t) + 2\xi\omega \cdot \dot{x}(t) + k_p\omega^2 \cdot x(t-\tau) = a(t) \tag{6}$$

where ξ and ω are the damping ratio and circular frequency of the SDOF structure, respectively; t is time function; $\dot{x}(t)$ and $\ddot{x}(t)$ are the velocity and acceleration responses of the SDOF

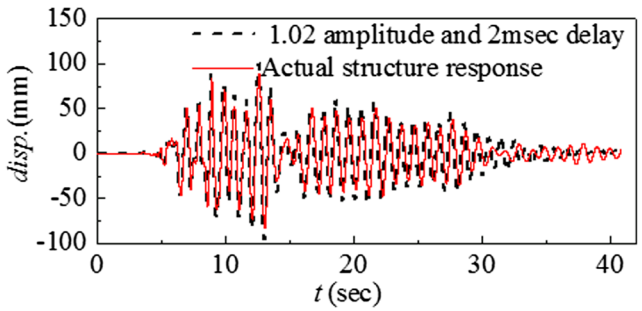

Fig. 7 The measured displacements for time delay of 2 msec. and amplitude error of 1.02

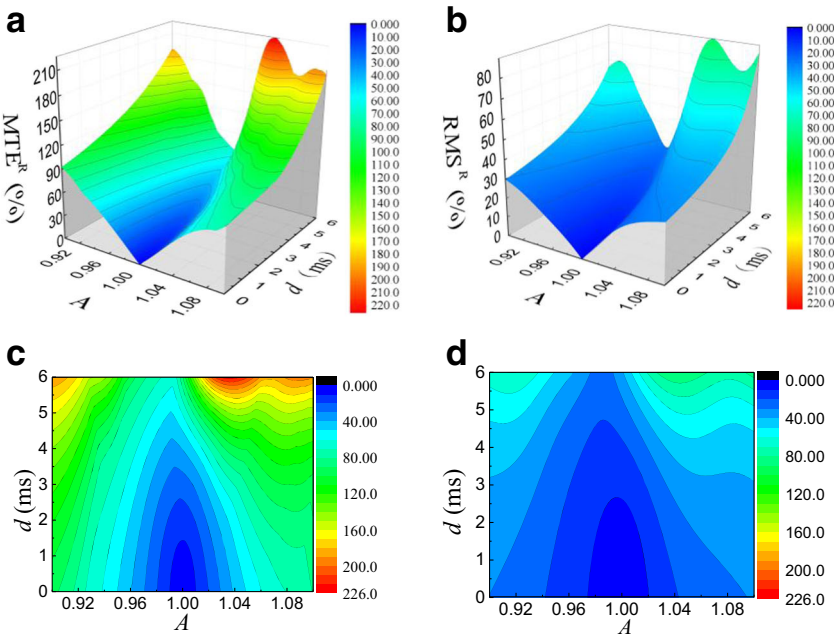

Fig. 8 Contour plot when amplitude error and time delay existed for (**a**) *MTER* (surface plot), **b**) *RMSR* (surface plot), (**c**) *MTER* (plain) and (**d**) *RMSR* (plain)

structure, respectively; $a(t)$ is the external excitation; and k_p and τ constants which represent the amplitude error and time delay due to servo-hydraulic dynamics in a real-time hybrid simulation, respectively. Based on equation (6), the structure response $x(t)$ depends on damping ratio, stiffness and external excitation. The influence of these factors on the accuracy of simulated structural responses can be derived by simulations of typical structures with different damping ratios and stiffness subjected to a suite of ground motions. Assuming these three factors are independent from each other, the correlation between simulation accuracy and FEI indices can be established. For illustration, the fundamental frequency of the structure is 1 Hz, and the inherent damping ratio is assumed to be 0.02. The NIS000 component of the 1995 Kobe earthquake recorded at Nishi-Akashi station is randomly selected from the PEER Strong Motion Database [29] for the simulation. The sampling rate for the computational simulation is assumed to be 1024 Hz, which is consistent with the state-of-the-art servo-hydraulic equipment. To accommodate different sampling rate from the ground motion records, a first order linear interpolation method is used for resampling the ground motion records in 1024 Hz.

The corresponding block diagram is presented in Fig. 1 for real-time hybrid simulation of a SDOF linear structure, where the stiffness k is isolated as the experimental substructure to calculate the restoring force by multiplying the measured displacements while the rest of the SDOF structure is modeled as the analytical substructure. The calculated displacements and measured displacements are denoted as x_c and x_m in Fig. 1, respectively, where the calculated displacements are used as input and measured displacements are considered as output in FEI in equation (1). The delay is represented by a transport delay τ while the possible amplitude error is represented by a proportional gain k_p [30].

For an ideal experiment, a compensation method can completely eliminate the amplitude error and time delay, i.e., the FEI indices A and d are equal to 1 and 0, respectively. The actual structural response can be calculated by setting time delay τ and amplitude k_p in

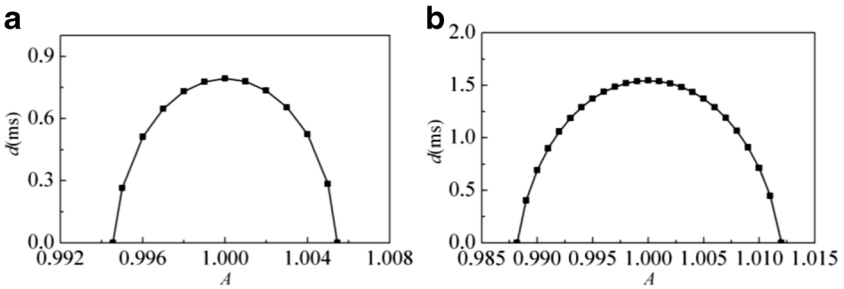

Fig. 9 The relationship between A and d with 5% error for (**a**) MTE^R and (**b**) RMS^R

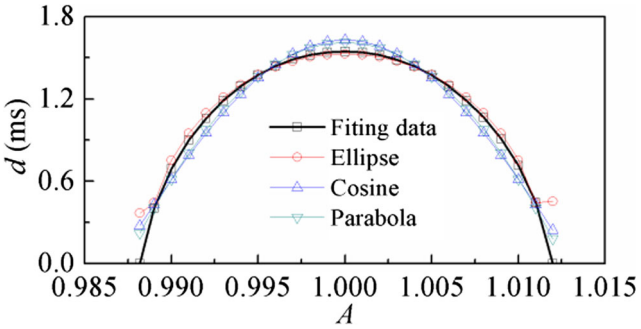

Fig. 10 Curve fitting for 5% RMS^R error

Fig. 1 to 0 and 1, respectively. In this case, both measured and calculated displacements are the same as actual structural responses, which are referred to as $x_1(t)$ in Fig. 2. It can be observed that the displacement response is relatively small during the first 5 seconds and increases from 7 to 13 sec.. The displacement between 14 and 30 sec. varies from -50mm to 50mm. The displacement then decreases gradually to smaller than 5mm after 40 sec..

Correlation Between Time Delay *d* and Test Accuracy

Computational simulations are conducted to quantify the correlation between time delay and simulation accuracy. For the purpose of analysis, the amplitude gain k_p is set to be 1. Since the critical delay for stability is 6.4 msec. for the SDOF structure with natural frequency of 1 Hz [9], the computational simulations select the time delay τ from 0.1 to 8 msec. with increment of 0.1 msec..

Figure 3 presents the measured displacements when time delay is 5 msec.. Compared with the actual response in Fig. 2, the peak value in Fig. 3 is around 50 mm at 40 sec. Figure 3 also shows the accumulative effect of time delay in real-time hybrid simulation, where the actuator delay would lead to inaccurate test results even the simulation remains stable.

Both the MTE^R and RMS^R errors in Fig. 4 are observed to increase linearly with respect to delay when time delay is less than 4 msec. and then exponentially when time delay is larger than 4 msec.. When the time delay is equal to 6.4 msec. of critical delay for stability, the MTE^R and RMS^R errors are calculated as 280% and 96%, respectively, which are obviously unacceptable for engineering applications. A new criterion is required for reliability assessment of real-time hybrid simulation in the presence of time delay.

Table 1 Fitting parameters and fitting error

Curve	*a*	*B*	error
Ellipse	1.3×10^{-4}	2.3	0.12
Cosine	1.6	118.5	0.65
Parabola	-1.0×10^{4}	1.6	0.42

Correlation Between Amplitude *A* and Simulation Accuracy

To quantify the relationship between amplitude error and test accuracy, the amplitude k_p varies from 0.98 to 1.02 with an increment of 0.001 while time delay τ remains 0. Figure 5 presents the measured displacements of the simulation when amplitude is 0.99. Compared with the actual structural response in Fig. 2, the displacements in Fig. 5 are almost exactly the same, implying that an amplitude error of 0.01 has little effect on the simulation accuracy.

Figure 6 shows the MTE^R and RMS^R errors for different amplitude errors. Both MTE^R and RMS^R are observed to increase linearly with respect to amplitude error when the amplitude error is less than 0.02. The slope for MTE^R is about two times larger than that of RMS^R in Fig. 6. For the simulation with the amplitude error of 1%, the MTE^R and RMS^R errors are 9.2% and 4.2%, respectively. Thus, the amplitude error is also cumulative in real-time hybrid simulation and should be accounted for reliability assessment.

From the analysis above, correlation between test errors and the FEI indices are explored for a linear elastic SDOF structure under one selected ground motion. The MTE^R and RMS^R of the simulation increase linearly for small time delay while exponentially for large time delay. One the contrary, the MTE^R and RMS^R of the simulation grow with amplitude error linearly when the amplitude error is less than 0.02. Due to the cumulative effect of time delay and amplitude error on real-time hybrid simulation, the results might be incredible even when the test is stable. A new criterion is necessary to account for the influence of both time delay and amplitude error for reliability assessment of real-time hybrid simulation results.

Criterion for Reliability Assessment

In most situations, both the amplitude error and the time delay exist between calculated and measured displacements in a real-time hybrid simulation. New simulations are conducted to account for simultaneous amplitude error and time delay. The time delay τ changes from 0 to 2msec for every 0.1msec while amplitude k_p varies from 0.98 to 1.02 for every 0.001. A total of 800 simulations are conducted for different combinations of amplitude error and time delay. Figure 7 shows the displacements of the simulation with time delay of 2msec and amplitude error of 0.02. The displacements in Fig. 7 are obviously larger than the ideal displacement with the maximum displacement about 10% larger than that in Fig. 2. The contour

Table 2 Fitting parameters and the fitting error for MTE^R

No.	Earthquake /Component	$a(10^{-4})$	b	error	No.	Earthquake /Component	$a(10^{-4})$	b	error
1	NORTHR/MUL009	0.67	1.35	0.03	51	SUPERST/B-PTS225	1.58	3.02	0.06
2	NORTHR/MUL279	0.76	1.51	0.03	52	SUPERST/B-PTS315	5.74	9.74	0.41
3	NORTHR/LOS000	1.01	2.02	0.04	53	LOMAP/STG000	1.53	2.55	0.21
4	NORTHR/LOS270	1.12	2.27	0.05	54	LOMAP/STG080	3.27	4.85	0.21
5	DUZCE/BOL000	3.20	4.47	0.39	55	ERZIKAN/ERZ-NS	1.54	2.79	0.08
6	DUZCE/BOL090	1.59	2.59	0.11	56	ERZIKAN/ERZ-EW	0.61	1.28	0.03
7	HECTOR/0542a090	1.21	2.19	0.13	57	CAPEMEND/PET000	0.45	0.90	0.04
8	HECTOR/0542c180	1.34	2.47	0.10	58	CAPEMEND/PET090	1.05	1.88	0.06
9	IMPVALL/H-DLT262	0.97	1.71	0.09	59	LANDERS/LCN260	1.38	2.38	0.15
10	IMPVALL/H-DLT352	1.15	1.93	0.06	60	LANDERS/LCN345	1.34	2.31	0.09
11	IMPVALL/H-E11140	1.86	2.99	0.19	61	NORTHR/RRS228	0.71	1.46	0.04
12	IMPVALL/H-E11230	12.60	24.98	0.99	62	NORTHR/RRS318	1.19	2.31	0.05
13	KOBE/NIS000	1.38	2.35	0.13	63	NORTHR/SYL090	1.72	2.82	0.13
14	KOBE/NIS090	1.32	2.31	0.07	64	NORTHR/SYL360	2.69	4.09	0.16
15	KOBE/SHI000	6.33	8.10	0.77	65	KOCAELI/IZT180.	0.48	0.99	0.02
16	KOBE/SHI090	1.11	2.13	0.09	66	KOCAELI/IZT090	1.44	2.59	0.09
17	KOCAELI/DZC180	3.33	6.46	0.70	67	CHICHI/TCU065-E	5.08	5.65	0.09
18	KOCAELI/DZC270	0.78	1.56	0.05	68	CHICHI/TCU065-N	1.44	2.38	0.17
19	KOCAELI/ARC000	1.07	2.15	0.04	69	CHICHI/TCU102-E	1.57	2.49	0.10
20	KOCAELI/ARC090	2.76	5.18	0.16	70	CHICHI/TCU102-N	1.63	2.53	0.21
21	LANDERS/YER270	1.93	4.41	0.06	71	DUZCE/DZC180	0.81	1.58	0.05
22	LANDERS/YER360	2.15	5.01	0.13	72	DUZCE/DZC270	0.71	1.43	0.04
23	LANDERS/CLW-LN	4.69	7.03	0.42	73	GAZLI/GAZ000	1.24	2.78	0.13
24	LANDERS/CLW-TR	1.99	3.69	0.09	74	GAZLI/GAZ090	0.83	1.84	0.03
25	LOMAP/CAP000	24.50	47.81	3.25	75	IMPVALL/H-BCR140	2.29	4.01	0.28
26	LOMAP/CAP090	0.88	1.74	0.10	76	IMPVALL/H-BCR230	1.13	2.22	0.05
27	LOMAP/G03000	0.77	1.46	0.04	77	IMPVALL/H-CHI012	0.80	1.68	0.07
28	LOMAP/G03090	2.46	3.84	0.16	78	IMPVALL/H-CHI282	1.62	3.54	0.17
29	MANJIL/ABBAR--L	1.37	2.47	0.16	79	NAHANNI/S1010	1.50	2.86	0.13
30	MANJIL/ABBAR--T	4.48	8.03	0.55	80	NAHANNI/S1280	0.68	1.38	0.03
31	SUPERST/B-ICC000	12.32	27.72	1.24	81	NAHANNI/S2240	0.57	1.25	0.05
32	SUPERST/B-ICC090	0.63	1.23	0.03	82	NAHANNI/S2330	1.62	3.02	0.21
33	SUPERST/B-POE270	2.02	4.45	0.09	83	LOMAP/BRN000	3.26	5.95	0.36
34	SUPERST/B-POE360	1.57	3.14	0.07	84	LOMAP/BRN090	2.43	4.45	0.11
35	CAPEMEND/RIO270	1.65	2.71	0.20	85	LOMAP/CLS000	0.79	1.47	0.06
36	CAPEMEND/RIO360	0.58	1.15	0.03	86	LOMAP/CLS090	2.43	4.31	0.17
37	CHICHI/CHY101-N	2.26	5.25	0.11	87	CAPEMEND/CPM000	1.03	1.90	0.05
38	CHICHI/CHY101-W	2.54	5.96	0.14	88	CAPEMEND/CPM090	2.23	3.79	0.13
39	CHICHI/TCU045-E	1.95	2.95	0.20	89	NORTHR/0637-270	3.12	4.98	0.31
40	CHICHI/TCU045-W	6.07	7.19	0.37	90	NORTHR/0637-360	2.22	3.36	0.17
41	SFERN/PEL090	1.73	2.97	0.30	91	NORTHR/STC090	1.46	2.91	0.09
42	SFERN/PEL180	2.42	4.32	0.23	92	NORTHR/STC180	2.17	3.81	0.19
43	FRIULI/A-TMZ000	3.73	5.32	0.27	93	KOCAELI/YPT060	3.60	5.54	0.61
44	FRIULI/A-TMZ170	1.50	2.49	0.16	94	KOCAELI/YPT330	2.76	4.26	0.41
45	IMPVALL/H-E06140	4.73	5.95	0.10	95	CHICHI/TCU067-E	2.61	3.91	0.25
46	IMPVALL/H-E06230	1.39	2.43	0.07	96	CHICHI/TCU067-N	7.39	7.96	0.52
47	IMPVALL/H-E07140	1.49	2.59	0.09	97	CHICHI/TCU084-E	2.99	3.90	0.35
48	IMPVALL/H-E07230	1.25	2.23	0.13	98	CHICHI/TCU084-N	5.23	8.42	0.41
49	ITALY/A-STU000	0.69	1.50	0.03	99	DENALI/ps10047	4.21	5.30	0.15
50	ITALY/A-STU0270	1.33	2.71	0.06	100	DENALI/ps10317	4.56	6.21	0.47

plots under different amplitude errors and time delays can be seen in Fig. 8.

To determine if the test results are reliable when the actual structural responses are unavailable or unknown for direct comparison, the amplitude error and time delay between calculated displacements and measured displacements are utilized to estimate whether the test error between ideal displacements and measured displacements are acceptable. In this study, a 5% error is selected for the purpose of illustration of presented methodology implying that the measured displacements are reliable if the error (MTE^R or RMS^R) is less than 5%. Figure 9 presents the FEI indices A and d for MTE^R and RMS^R equal to 5% for linear structure with natural frequency of 1 Hz subjected to the selected ground motion. The curves in Fig. 9(a) and (b) are calculated by taking 5% as threshold value for reliability assessment, and can be easily extended to other values depending on the different requirements of the researchers. The curves in Fig. 9 can be considered as the criterion to determine the reliability of real-time hybrid simulation for the selected ground motion. If the indices A and d calculated are located inside the curve in Fig. 9(a) and (b), the MTE^R or RMS^R between measured displacements and actual responses is less than 5%, otherwise the error is larger than 5%. The reliability of real-time hybrid simulation can thus be determined using the FEI indices. It can also be observed in Fig. 9 that MTE^R presents more stringent requirement on time delay and amplitude error than the RMS^R. However, this could be

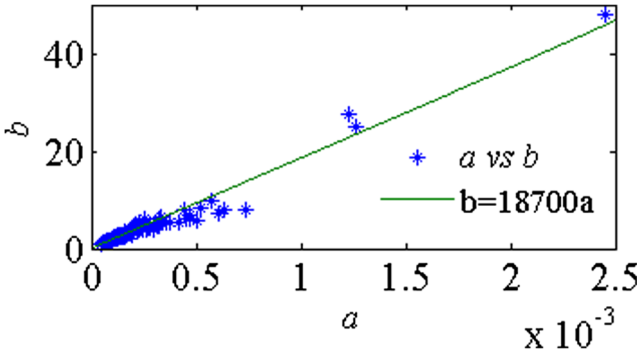

Fig. 11 Correlation between parameters *a* and *b*

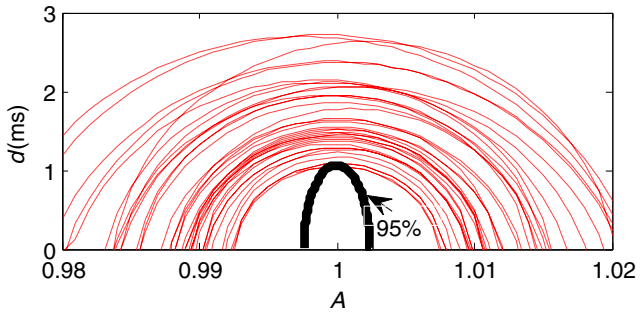

Fig. 13 Criterions with 95% guarantee rate for different ground motions

difficult to fulfill in real-time hybrid simulation. The curve in Fig. 9(b) is therefore used in this study to evaluate the performance of real-time hybrid simulation with the presented methodology.

Curve Fitting

The curve in Fig. 9(b) is fitted into a function for the purpose of practical application so that the reliability of the tests can be evaluated. The curve fitting in this study is based on the criterion that the parameters in target function should be as few as possible while the results should be as accurate as possible. Three functions including ellipse, cosine and parabola are used to fit the curve. The center of ellipse is located in (*A*, *d*) equal to (1, 0), the symmetry axis of cosine and parabola curves locate at *A* equal to 1. The equations of these three functions are expressed as following:

$$\frac{(A-1)^2}{a'^2}+\frac{d^2}{b'^2}=1 \tag{7a}$$

$$d=a\cos(b(A-1)) \tag{7b}$$

$$d=a(A-1)^2+b \tag{7c}$$

where a, a', b and b' are the constants to be determined.

Equation (7a) can also be written as:

$$d=\pm b'^2\cdot\sqrt{1-\frac{(A-1)^2}{a'^2}} \tag{8}$$

In equation (8), d represents time delay, which is a real value. For this reason, the absolute value of A-1 should be less than a'. However, a' is the parameter to be determined, which is impossible to guarantee in data fitting. So equation (7a) is rewritten into the following form:

$$d'=\left(a\cdot b-b\cdot A'\right)/a \tag{9}$$

where d' represents the square of d, A' represents the square of $(A\text{-}1)$;a represents the square of a'; b represents the square of b'. The index to evaluate the fitting performance is calculated by the following equation:

$$error=\sum_{i=1}^{n}\left(\overline{d}_i^2-d_i'\right)^2 \tag{10}$$

where $\overline{d}$ is the time delay calculated by fitting equation; n represents the number of data and equals 25 in this function.

MATLAB Curve Fitting Toolbox [30] is used to determine the parameters as shown in Fig. 10. The corresponding values of the parameters and the fitting errors are presented in Table 1. The ellipse function is observed to lead to smallest error and therefore is considered to be the best fit. The reliability criterion of the real-time hybrid simulation can be written as:

$$\frac{(A-1)^2}{1.3\times10^{-4}}+\frac{d^2}{2.3}\le1 \tag{11}$$

When A and d of a real-time hybrid simulation satisfy equation (11), the RMS^R between simulated displacements and actual structural responses would be less than 5%. The

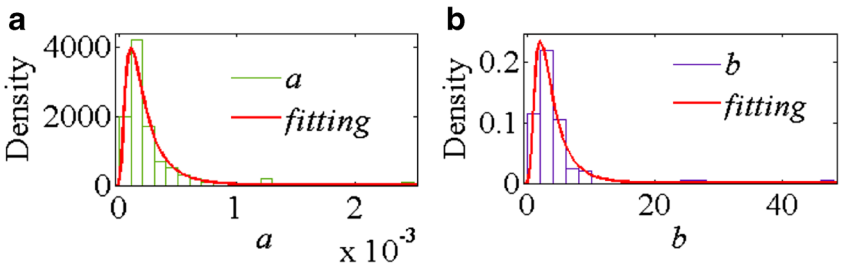

Fig. 12 Lognormal distributions for (**a**) *a* and (**b**) *b*

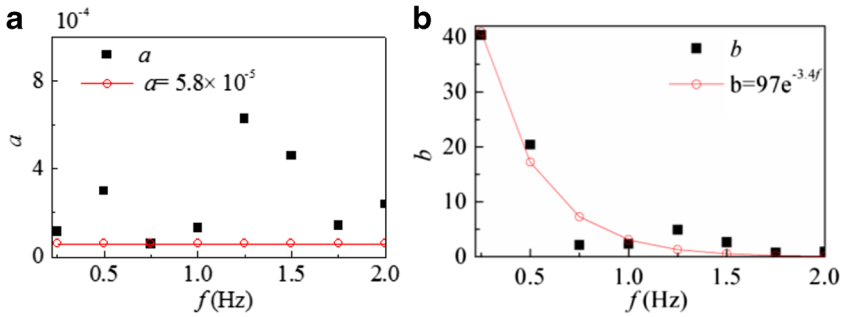

Fig. 14 Parameters for different frequencies for ground motion NIS000 for (**a**) *a* and (**b**) *b*

test results are therefore considered reliable for truthfully replicating the structural response of the SDOF structure under the selected ground motion. Otherwise, the results are considered not reliable due to larger RMS^R than 5%.

Probabilistic Approach for Reliability Analysis Under Different Ground Motions

The reliability criterion in equation (11) is derived considering the NIS000 component of the 1995 Kobe earthquake as input. To further extend this proposed methodology, a suite of ground motions are selected to calculate the parameters *a* and *b* in equation 7(a). Due to different characteristics of various ground motions, it is naturally expected that different sets of *a* and *b* are statistically derived. The parameters *a* and *b* with 95% confidence are selected based probability and statistical theory. The reliability criterion with selected *a* and *b* is expected to evaluate the accuracy of real-time hybrid simulation for the worst-case scenarios.

Ellipse Parameters Under Different Ground Motions

In this paper, twenty four sets of far-field ground motions as well as twenty eight near-field ground motions are selected from the PEER Strong Motion Database [24]. Two components of each earthquake are analyzed to calculate the parameters *a* and *b* which are presented in Table 2, where the parameter *a* varies from 5.5×10^{-5} to 6.6×10^{-4} corresponding to the amplitude error from 7.4×10^{-3} to 2.3×10^{-2}. The parameter *b* varies from 1.1 to 7.6, which corresponds for time delay from 1.05 msec. to 2.76 msec.

The values of parameters *a* and *b* are presented in Fig. 10 for different ground motions. It can be observed that *b* increases almost linearly with respect to *a*. The correlation coefficient of 0.9774 between *a* and *b* indicates strong dependence between these two parameters. Using linear polynomial model, the results can also be observed in Fig. 11. From Fig. 11, *b* is about 1.65×10^4 times larger than *a*.

Probabilistic Approach for Reliability Analysis

Different excitations can derivate different *a* and *b*, but these parameters are almost proportional for the same frequency and damping. To get the reliability criterion, MATLAB statistic toolbox [30] is used to fit the parameters of *a* and *b* into lognormal distribution as shown in Fig. 12. The parameters with 95% confidence are selected as criterion.

In Fig. 12(a), the parameter *a* varies from 0.5×10^{-4} to 4.5×10^{-4} with peak value around 1×10^{-4}. The 95% confidence for *a* gives 5.3×10^{-5}, which represents the boundary amplitude error for 5% RMS^R is about 0.0073. In Fig. 12(b), *b* varies from 1 to 7 with peak value around 2. The 95% confidence for *b* gives 1.04, which indicates that the critical delay for 5% RMS^R is about 1.02 msec. Thus, the reliability boundary of the real-time hybrid simulation for 100 strong ground motions can be written as:

$$\frac{(A-1)^2}{5.3 \times 10^{-5}} + \frac{d^2}{1.04} \le 1 \tag{12}$$

The curve fitting for different ground motions and the curve with 95% confidence are presented in Fig. 13. It is observed that different ground motion input lead to different eclipse functions, implying that it

Table 3 The parameter for both *a* and *b* with 95% guaranteed rate under different frequency

f	0.25Hz	0.5Hz	0.75Hz	1Hz	1.25Hz	1.5Hz	1.75Hz	2Hz
a	6.6×10^{-5}	4.6×10^{-5}	4.3×10^{-5}	5.8×10^{-5}	6.2×10^{-5}	5.1×10^{-5}	5.8×10^{-5}	7.3×10^{-5}
b	23.27	4.01	1.62	1.13	0.83	0.44	0.38	0.33

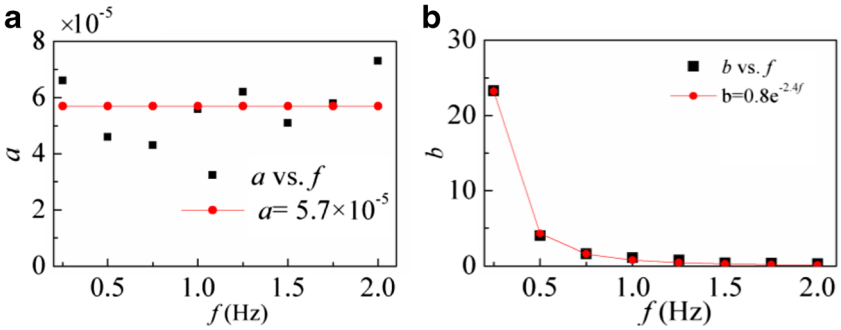

Fig. 15 Data fitting for (**a**) a and (**b**) b

would be difficult, if not impossible, to assess the reliability of the real-time hybrid simulation results in a deterministic manner.

The Influence of Frequency

Previous study by Wallace et al. [7] shows that the critical delay for stability is dependent on the frequency of the structure. It is necessary for the reliability criterion to account for the influence of different frequencies. The same block diagram in Fig. 1 is used for computational simulation. Different frequencies of the structure are used including1.0 Hz, 0.25 Hz, 0.5 Hz, 0.75 Hz, 1 Hz, 1.25 Hz, 1.5 Hz, 1.75 Hz and 2 Hz with the other parameters unchanged. Following the same procedure as described above, the parameters a and b in equation (9) are derived for each frequency and presented in Fig. 14.

It can be observed from Fig. 14(a) that a changes randomly with frequency, which means the frequency has little influence on a. The parameter a is observed to vary from 5.8×10^{-5} to 7×10^{-4}, which corresponds to the amplitude error 0.008 and 0.027, respectively. On the contrary, parameter b shows a strong dependence on frequency in Fig. 14(b) to decrease quickly with respect to frequency smaller than 0.75Hz. This observation is consistent with the maximum allowable delay calculated by Gao et al. [22], which the allowable delay decrease dramatically with the increase of the frequency. The parameter b varies from less than 0.8 to 40.4, which corresponds to the time delay of 0.9 msec. and 6.4 msec., respectively. For simplification, the minimum of parameter a in Fig. 14(a) is selected while the parameter b fits into an exponential function with frequency, which is assumed as:

$$b = k_1 e^{-k_2 f} \tag{13}$$

The results from the curve fitting are presented in Fig. 14. The reliability criterion of the real-time hybrid simulation for the NIS000 component of the 1995 Kobe earthquake can be rewritten as:

$$\frac{(A-1)^2}{5.8 \times 10^{-5}} + \frac{d^2}{97e^{-3.4f}} \le 1 \tag{14}$$

To account for the influence of different ground motions, the parameters for both a and b with 95% confidence under 0.25 Hz, 0.5 Hz, 0.75 Hz, 1.25 Hz, 1.5 Hz, 1.75 Hz and 2 Hz are derived and presented in Table 3. Similar to that observed in Fig. 15, the parameter of a changes with respect to frequency while b shows a strong dependence on frequency. Since the frequency has little influence on a, the parameter a can be calculated based on all the parameters under different frequencies to get more reliable results. The parameter for a with 95% confidence under different frequencies is 5.6×10^{-5}. The parameter b also fits into an exponential function with frequency in equation (13) as shown in Fig. 15.

The reliability criterion for the real-time hybrid simulation in worst-case scenario for the damping ratio of 0.02 can be written as:

$$\frac{(A-1)^2}{5.6 \times 10^{-5}} + \frac{d^2}{121.6e^{-6.6f}} \le 1 \tag{15}$$

It can be observed in equation (15) that the frequency has little influence on the boundary of amplitude error but plays an important role in the boundary of time delay. To ensure the reliability of real-time hybrid simulation, amplitude error should be less than 0.0073 in worst-case scenario. In other words, the RMS^R

Table 4 The parameter for both a and b under different damping ratio

ξ	0.02	0.03	0.04	0.05	0.06	0.07	0.08	0.09	0.10
a	1.3×10^{-4}	4.3×10^{-4}	8.3×10^{-4}	1.3×10^{-3}	1.9×10^{-3}	2.8×10^{-3}	3.8×10^{-3}	4.9×10^{-3}	6.1×10^{-3}
b	1.7	2.8	3.9	5.0	6.0	7. 3	8.5	9.6	10.7

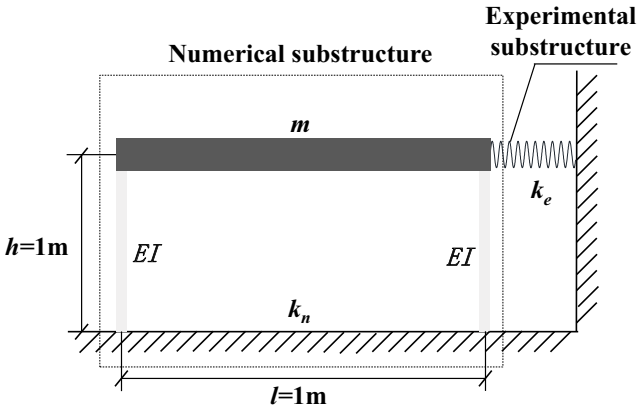

Fig. 16 Model structure in numerical simulation

between measured displacements and the ideal displacements would be larger than 5% if A is larger than 1.0073 or smaller than 0.9927, no matter how small the time delay is in the test. On the contrary, the test results may be reliable even the time delay is as large as 4.8 msec. when the frequency is 0.25 Hz, but may be unreliable when this delay is 0.6 msec. for 2 Hz. The higher frequency of the structure, the more accurate delay compensation method should be used.

The Influence of Damping Ratio

Besides the ground motion and frequency, the damping ratio has also been shown to affect the critical time delay for real-time hybrid simulation. For the same linear elastic SDOF structure with natural frequency of 1.0 Hz, the damping ratio is varied from 0.02 to 0.10 with an increment of 0.01. Following the same procedures described above, a and b are derived for each damping ratio for the NIS000 component of the 1995 Kobe earthquake and presented in Table 4. It can be observed that both a and b increase linearly with damping ratio, which can be expressed as linear functions of damping ratio as following:

$$a = k_3\xi \tag{16a}$$

$$b = k_4\xi \tag{16b}$$

The parameters of k_3 and k_4 are found to be 0.046 and 100, respectively, for the simulation with the ground motion NIS000. The criterion for the NIS000 component of the 1995 Kobe earthquake when the structure is 1 Hz can be written as:

$$\frac{(A-1)^2}{0.046\xi} + \frac{d^2}{100\xi} \le 1 \tag{17}$$

Though equations (16a) and (16b) are calculated based on NIS000 component of the 1995 Kobe earthquake and 1 Hz structure, other ground motions and frequency also follow the same relationship between parameters in ellipse and damping ratios since the damping ratio is independent with ground motion and frequency.

To account for the influence of ground motions, a and b can be calculated based on equations (11), (15) and (17). Comparing equation (11) with equation (17) for a, $1.3 \times 10\text{-}4$ is equal to 0.046ξ, then $5.6 \times 10\text{-}5$ in equation (15) is equal to 0.021ξ. Comparing equation (11) with equation (17) for b, 2.3 is equal to 1000ξ, then $121.6e^{-6.6f}$ in equation (15) is equal to $46080\xi e^{-6.6f}$. The criterion therefore can be formulated as

$$\frac{(A-1)^2}{0.021\xi} + \frac{d^2}{6080\xi e^{-6.6f}} \le 1 \tag{18}$$

The RMS^R between measured displacements and the actual responses would be less than 5% if the A and d between calculated displacements and measured displacements satisfy equation (18).

Application of the Criterion

Numerical simulations are conducted to demonstrate the effectiveness of the proposed criterion in equation (18). The model structure for RTHS is a SDOF frame with a spring as shown in Fig. 16, of which the frame is taken as numerical substructure and the spring is considered as the experimental substructure. The mass and the stiffness of the frame are m and k_n, while the stiffness of the spring is k_e. Four different cases of

Table 5 Parameters in each case

case	f_n (Hz)	ξ	K_e (N/m)	k_n (N/m)	$m = (k_e + k_n)/(2\pi f_n)^2$ (kg)	$EI = k_n h^3/24$ (N · m^2)	EA (N · m^2)	α_{es}	Amplitude error
1	1	0.02	3.50	1E-6	0.09	4.17E-8	4.17E-3	3.6	1.0037
2	0.6	0.02	3.50	1E-6	0.25	4.17E-8	4.17E-3	2.7	1.0035
3	1	0.05	3.50	1E-6	0.09	4.17E-8	4.17E-3	3.4	1.0117
4	1	0.02	3.50	1E-6	0.09	4.17E-8	4.17E-3	3.2	1.0074

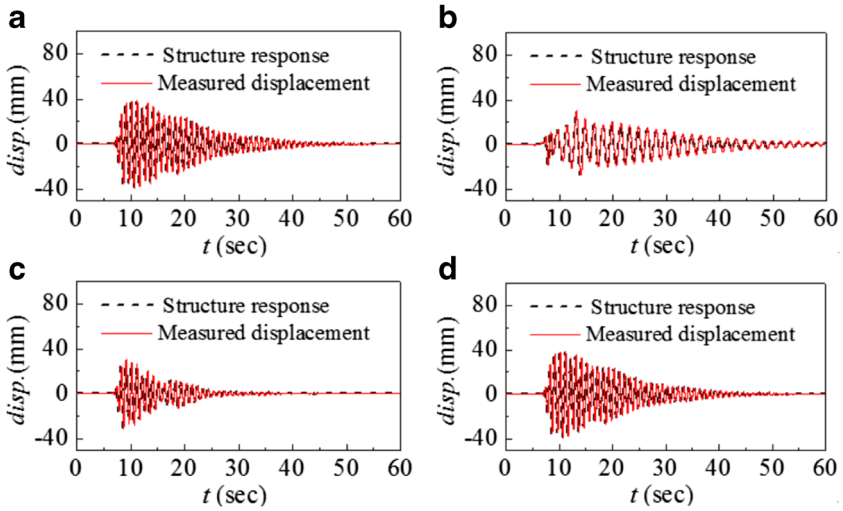

Fig. 17 Structure response in first simulation and measured displacement in second simulation for (**a**) case 1, (**b**) case 2, (**c**) case 3 and (**d**) case 4

simulations are conducted to account for difference natural frequencies, damping ratios as well as different values of FEI indices. Numerical simulations presented herein are conducted using Frame_2D [31], where the CR integration algorithm [7] is used to compute the structure responses. The parameters of the numerical simulations are tabulated in Table 5. From Table 5, k_e and k_n are 3.50 N/m and 1×10^{-6} N/m respectively for all cases. Thus, the stiffness of the structure can be considered as concentrated in experimental substructure. The KJM000 component of the 1995 Kobe earthquake is selected as the external excitation with the peak ground motion acceleration of 0.707g, which is not used in previous statistical analysis. A time delay of 4 msec. is assumed for the actuator dynamics for all numerical simulations, and the inverse compensation [13] is used for delay compensation with the α_{es} also presented in Table 5. The simulated structural responses are compared with exact responses in Fig. 17. The RMS^R error of the simulated structural responses as well as FEI indices are calculated and presented in Table 6.

The amplitude and time delay indices in Table 6 can be substituted into equation (18) for reliability assessment. The first three cases satisfy the criterion for 5% RMS^R error while the fourth case does not, which indicates the first three cases could be considered reliable but the fourth case could have larger RMS^R error than 5%. On the other hand, RMS^R errors between simulated structural and exact responses are observed to be smaller than 5% for first three cases but larger than 5% for the fourth case, which are consistent with the assessment using equation (18), implying that the criterion is effective.

Summary and Conclusions

Since the actuator delay cannot be completely eliminated by existing compensation methods, post-simulation reliability assessment is necessary for real-time hybrid simulation. Determining the reliability of the simulation remains a challenge even a number of evaluation methods have been proposed. In this paper, correlation between the FEI indices and the reliability of the test is established by an ellipse for the worst-case scenarios, where the RMS^R response error is fixed to find the corresponding tracking errors. Probabilistic and statistical methods based on the simulation of one hundred earthquake components are used to account for the effect of various ground motion inputs, different natural frequencies and damping ratios. Different from stability analysis under actuator delay, the influence of amplitude error is also considered based on the observations in previous experimental studies. A 5% RMS^R error is used to demonstrate the proposed methodology for reliability assessment through the FEI indices derived through the calculated and measured displacements. Simulations are conducted to reveal the application of this criterion.

Table 6 FEI indices and RMS^R

case	A	d	$(A\text{-}1)^2/(0.021\xi) + d^2/(6080\xi e^{-6.6f})$	fulfill equation (18)	RMS^R (%)
1	1.0039	0.39	0.956	Yes	2.55
2	1.0036	1.30	0.760	Yes	3.16
3	1.0119	0.59	0.977	Yes	2.00
4	1.0080	0.78	3.830	No	5.35

Studies presented herein show that parameters a and b of the ellipse function are linearly correlated when the frequency of the structure is fixed, indicating that the external excitation and damping ratio can influence the reliability boundary for both amplitude error and time delay. On the other hand, the frequency has little effect on amplitude reliability boundary but can significantly influence delay reliability boundary. The criterion presented in equation (18) can be used as post-test reliability assessment of RHTS results. The test can be considered reliable if time delay and amplitude errors satisfy the proposed criterion. Numerical simulations are conducted to demonstrate the effectiveness of the proposed reliability criterion. Besides, the criterion can be also used to design RTHS, which the tolerance amplitude error and time delay can be estimated before test. For the future work, the reliability criterion should consider cases other than worst-case to provide more accurate assessment of real-time hybrid simulation. The reliability criterion should be also further extended to nonlinear structures and multiple degrees of freedom structures.

Acknowledgements The authors would like to acknowledge the support from National Science Foundation of China under grant No.51378107, the Fundamental Research Funds for the Central Universities and Doctoral Research Fund by Southeast University under Grant No. YBJJ-1442, and National Science Foundation under the grant number CMMI-1227962.

References

1. Asai T, Chang CM, Spencer BF (2014) Real-time hybrid simulation of a smart base-isolated building. J Eng Mech 141(3):04014128
2. Chen C, Ricles JM, Sause R, Christenson R (2010) Experimental evaluation of an adaptive inverse compensation technique for real-time simulation of a large-scale magneto-rheological fluid damper. Smart Mater Struct 19(2):025017
3. Shao X, Enyart G (2014) Development of a versatile hybrid testing system for seismic experimentation. Exp Tech 38(6):44–60
4. Shao X, Griffith C (2013) An overview of hybrid simulation implementations in NEES projects. Eng Struct 56:1439–1451
5. Nakashima M, Kato H, Takaoka E (1992) Development of real-time pseudo dynamic testing. Earthq Eng Struct Dyn 21(1):79–92
6. Wu B, Xu G, Wang Q, Williams MS (2006) Operator-splitting method for real-time substructure testing. Earthq Eng Struct Dyn 35(3):293–314
7. Chen C, Ricles JM, Marullo T, Mercan O (2009) Real-time hybrid testing using the unconditionally stable explicit CR integration algorithm. Earthquake Eng Struct Dynam 38(1):23–44
8. Horiuchi T, Inoue M, Konno T, Namita Y (1999) Real-time hybrid experimental system with actuator delay compensation and its application to a piping system with energy absorber. Earthquake Eng Struct Dynam 28(10):1121–1141
9. Wallace MI, Sieber J, Neild SA, Wagg DJ, Krauskopf B (2005) Stability analysis of real-time dynamic substructuring using delay differential equation models. Earthquake Eng Struct Dynam 34(15):1817–1832
10. Chen C, Ricles JM (2009) Analysis of actuator delay compensation methods for real-time testing. Eng Struct 31(11):2643–2655
11. Horiuchi T, Knno T (2001) A new method for compensating actuator delay in real–time hybrid experiments. Philosophical Trans Royal Soc London A: Math Phys Eng Sci 359(1786):1893–1909
12. Ding Y, Wang Z, Wu B, Bursi OS, Xu G (2014) An effective online delay estimation method based on a simplified physical system model for real-time hybrid simulation. Smart Struct Syst 14(6):1247
13. Chen C, Ricles JM (2010) Tracking error-based servohydraulic actuator adaptive compensation for real-time hybrid simulation. J Struct Eng 136(4):432–440
14. Chen C, Ricles JM, Guo T (2012) Improved adaptive inverse compensation technique for real-time hybrid simulation. J Eng Mech 138(12):1432–1446
15. Phillips BM, Spencer BF (2012) Model-based multiactuator control for real-time hybrid simulation. J Eng Mech 139(2):219–228
16. Chae Y, Karim K, Ricles JM (2013) Adaptive time series compensator for delay compensation of servo-hydraulic actuator systems for real-time hybrid simulation. Earthquake Eng Struct Dynam 42(11):1697–1715
17. Mosqueda G, Stojadinovic B, Mahin SA (2007) Real-time error monitoring for hybrid simulation. part I: methodology and experimental verification. J Struct Eng 133(8):1100–1108
18. Mercan O, Ricles JM (2007) Stability and accuracy analysis of outer loop dynamics in real-time pseudodynamic testing of SDOF systems. Earthquake Eng Struct Dynam 36(11):1523–1543
19. Hessabi RM, Mercan O (2012) Phase and amplitude error indices for error quantification in pseudodynamic testing. Earthquake Eng Struct Dynam 41(10):1347–1364
20. Guo T, Chen C, Xu W, Sanchez F (2014) A frequency response analysis approach for quantitative assessment of actuator tracking for real-time hybrid simulation. Smart Mater Struct 23(4):045042
21. Guo T, Xu W, Chen C (2014) Analysis of decimation techniques to improve computational efficiency of a frequency-domain evaluation approach for real-time hybrid simulation. Smart Struct Syst 14(6):1197–1220
22. Gao X, Castaneda N, Dyke SJ (2013) Real time hybrid simulation: from dynamic system, motion control to experimental error. Earthquake Eng Struct Dynam 42(6):815–832
23. Mercan O, Ricles JM (2008) Stability analysis for real-time pseudodynamic and hybrid pseudodynamic testing with multiple sources of delay. Earthquake Eng Struct Dynam 37(10):1269–1293
24. Zhu F, Wang J, Jin F, Chi F, Gui Y (2015) Stability analysis of MDOF real-time dynamic hybrid testing systems using the discrete-time root locus technique. Earthquake Eng Struct Dynam 44(2):221–241
25. Maghareh A, Dyke SJ, Prakash A, Rhoads JF (2014) Establishing a stability switch criterion for effective implementation of real time hybrid simulation. Smart Struct Syst 14(6):1221–1245
26. Maghareh A, Dyke S, Rabieniaharatbar S (2016) Predictive stability indicator: a novel approach to configuring a real-time hybrid simulation. Earthquake Eng Struct Dynam. doi:10.1002/eqe
27. Harris FJ (1978) On the use of windows for harmonic analysis with the discrete Fourier transform. Proc IEEE 66(1):51–83
28. Chen C, Valdovinos J, Santiallno H (2013) Reliability assessment of real-time hybrid simulation results for seismic hazard mitigation. Structures Congress, May 2-4, Pittsburgh, PA
29. PEER (2005) http://peer.berkeley.edu/
30. Guide MU (1998) The MathWorks Inc. Natick, MA 4:382
31. Castaneda N, Gao X, Dyke SJ (2012) RT-Frame2D: a computational platform for the real-time hybrid simulation of dynamically-excited steel frame structures. http://nees.org/resources/realtimeframe2d